Available online at www.sciencedirect.com
SCIENCE DIRECT®
C. R. Geoscience 335 (2003) 709–719
COMPTES RENDUS GEOSCIENCE

Geodynamics

Discovery of the Paleo-Tethys residual peridotites along the Anyemaqen–KunLun suture zone (North Tibet)

Elena A. Konstantinovskaia [a], Maurice Brunel [b,*], Jacques Malavieille [b]

[a] *Geological Institute, Russian Academy of Sciences, 7, Pyzhevsky per., 119 017 Moscow, Russia*
[b] *Laboratoire de dynamique de la lithosphère, UMR 5573, université Montpellier-2, cc 60, place Eugène-Bataillon, 34095 Montpellier cedex 5, France*

Received 24 June 2002; accepted 10 June 2003

Presented by Jean Dercourt

Abstract

The spinel peridotite from the Anyemaqen suture contains ⩾5% residual clinopyroxene and is characterized by a high abundance of the magmaphile elements Fe, Al and Ti in the primary mineral phases. Our data demonstrate that this rock represents residual mantle material, which has been affected by less than 10% partial melting prior to its emplacement. Its textural features indicate that the rock has been plastically deformed in a non-coaxial regime under lithospheric physical conditions at a relatively cool thermal regime below solidus temperature. We suggest that the peridotites from the Anyemaqen suture represent mantle material, which was either emplaced during incipient rifting on the Palaeozoic passive margin of Asia, or uplifted at slow spreading ridge setting in Paleo-Tethyan Ocean. Further researches are needed to make a definite choice between these two alternatives. ***To cite this article: E.A. Konstantinovskaia et al., C. R. Geoscience 335 (2003).***

Résumé

Découverte de péridotites résiduelles, témoins de l'océan Paléo-Téthys, dans la suture Anyemaqen–KunLun (Nord Tibet). Une péridotite à clinopyroxène et spinelle bien conservée a été découverte dans la suture d'Anyemaqen. C'est une lherzolite pauvre en clinopyroxène résiduel (⩾5%). La teneur en éléments tels que Al, Ti, et Fe est très élevée dans les minéraux primaires de cette roche. Ses caractéristiques chimiques montrent qu'il s'agit de matériel du manteau supérieur résiduel, qui a subi moins de 10% de fusion partielle avant sa mise en place. La texture mylonitique de cette péridotite montre que cette roche a été déformée par fluage plastique cisaillant non coaxial dans la lithosphère inférieure, dans des conditions *subsolidus* de basse température. Nous proposons que les péridotites de la suture d'Anyemaqen représentent le matériel du manteau supérieur, exhumé, soit pendant les stades initiaux de *rifting* de la marge passive paléozoïque de l'Asie, soit au niveau d'une dorsale océanique à vitesse lente de l'océan Paléo-Téthys. Si des recherches supplémentaires sont nécessaires pour discriminer ces deux possibilités, la découverte de ce type de roche révèle néanmoins l'existence incontestable de fragments d'une croûte océanique paléozoïque sur cette transversale du Kunlun. ***Pour citer cet article : E.A. Konstantinovskaia et al., C. R. Geoscience 335 (2003).***

* Corresponding author.
E-mail address: brunel@dstu.univ-montp2.fr (M. Brunel).

1631-0713/$ – see front matter
doi:10.1016/S1631-0713(03)00118-4

Keywords: lherzolite; KunLun; Tibet; Paleo-Tethys Ocean; oceanic residual peridotite; mantle material; plastic deformation

Mots-clés : lherzolite ; KunLun ; Tibet ; océan Paléo-Téthys ; peridotite océanique résiduelle ; matériel mantellique ; déformation plastique

Version française abrégée

1. Introduction

La zone de suture d'Anyemaqen s'étend sur une distance de 1200 km le long de la bordure nord-est du Tibet. Elle sépare les terrains triasiques de la chaîne de Songpan–Garze située au sud, du bloc du Qaidam au nord (Fig. 1a) [22,24,33]. La question cruciale pour la géodynamique de cette région est de savoir si cette suture représente réellement la trace de l'océan téthysien paléozoïque.

La suture présente une association péridotites–gabbros–ophicalcites–radiolarites, qui est typique et comparable à des séries ophiolitiques connues dans les Alpes et le long de la marge Ibérique [1–3, 19–21,23]. Elle contient des blocs de taille et de composition variées, qui représentent des fragments de lithosphère dont l'origine océanique paléo-téthysienne est contestable en raison de leur transformation et altération postérieures.

La discussion sur la nature (composition chimique) et l'origine même des ophiolites de la suture d'Anyemaqen provient aussi du fait qu'elles sont essentiellement connues à partir des données des roches volcaniques [27,33]. C'est pourquoi l'analyse des roches qui représentent les parties les plus profondes de la croûte inférieure et du manteau supérieur est indispensable.

Nous présentons, dans cette étude, les premières données obtenues pour cette région sur la composition chimique des minéraux résiduels contenus dans les péridotites d'Anyemaqen.

2. Contexte géologique

Au sein d'une matrice très déformée composée par le flysch triasique, on distingue, d'une part, des blocs de roches ophiolitiques d'âge Permien inférieur à Trias moyen et des carbonates bioclastiques d'âge Permien inférieur [6]. Ces roches d'origines différentes sont des lentilles tectoniques mises en contact lors de la réactivation tertiaire de la faille du Kunlun.

Nous avons analysé des péridotites provenant d'une écaille tectonique coincée le long de la faille du Kunlun, dans la région à l'ouest de Huashexia, au sud du lac de Tong Xi Tso (Fig. 1a). Dans ce secteur, la séquence ophiolitique d'une épaisseur de 300 m est composée en majorité par des péridotites serpentinisées, des flaser gabbros et amphibolites auxquels sont associés des lambeaux tectoniques, composés de quartzites, d'argilites et de radiolarites (Fig. 1b). Les roches de cette coupe sont fortement mylonitisées dans des bandes étroites, qui séparent des domaines dans lesquels les roches sont mieux préservées. Des veines d'ophicalcite affleurent au sein des péridotites et des gabbros. Au nord des ophiolites, les calcaires benthiques du Permien inférieur appartiennent aussi à des unités tectoniques lenticulaires ; ils sont datés par des microfossiles d'affinité Angara, qui indiquent un environnement de plate-forme interne (D. Vachard, comm. pers.).

3. La péridotite de la suture Anyemaqen

Un échantillon de péridotite exceptionnellement bien préservé des déformations et rétromorphoses secondaires a été découvert et sélectionné pour des analyses détaillées. Cette roche contient seulement 5% de serpentine. Sa composition modale est de $\geqslant$5% de clinopyroxène (Cpx) résiduel, 25% d'orthopyroxène (Opx), $\leqslant$68% d'olivine (Ol) et 2% de spinelle (Sp), ce qui correspond à une transition entre une harzburgite riche en clinopyroxène et une lherzolite à spinelle pauvre en clinopyroxène. La foliation mylonitique est bien marquée. Les lamelles d'exsolution de Cpx dans les grands (jusqu'à 1 cm) porphyroclastes d'Opx étirés sont parallèles aux plans de cisaillement, et obliques à l'allongement de l'Opx qui donne la foliation (Fig. 2A–C). Les porphyroclastes de Cpx sont petits (190–380 µm, rarement jusqu'à 600 µm) et fortement résorbés par une néo-blastèse en mosaïque de grains de Ol et de Sp (Fig. 2D et E). La texture mylo-

nitique de la roche est aussi soulignée par des bandes de Ol recristallisées, étendues parallèlement à l'alignement de porphyroclastes de Opx et de grains de Sp allongés (Fig. 2F).

4. Discussion et conclusion

Cette étude suggère que les péridotites de la suture d'Anyemaqen caractérisent le matériel du manteau supérieur, qui a subi moins de 10% de fusion partielle avant sa mise en place (Fig. 3c et d) [14]. La teneur en éléments tels que Al, Ti, et Fe est très élevée dans les minéraux résiduels de la péridotite étudiée, ce qui la rend très semblable aux péridotites résiduelles de dorsales océaniques à vitesse lente (Fig. 3a–d, Tableau 1) [9,15,16,28,29] et aux péridotites de la marge de Galice [10,13] et de l'île de Zabargad [5]. La composition chimique des minéraux et l'analyse texturale des péridotites d'Anyemaqen (texture de l'Ol et obliquité des Opx) montrent que ces roches ont subi une déformation plastique en cisaillement ductile non coaxiale dans des conditions *subsolidus* de basse température (800–1000 °C) et une forte contrainte déviatorique [25], suivie d'un stade de re-équilibration en base de lithosphère. Une déformation fragile tardive affecte les lherzolites et les gabbros. On distingue dans les roches des fractures multiples remplies par de la serpentine et des carbonates, ainsi que des veines d'ophicalcite et des brèches carboniques.

En conclusion, nous proposons que les péridotites de la suture d'Anyemaqen sont des représentants du manteau supérieur exhumés, soit pendant les stades initiaux de *rifting* de la marge passive paléozoïque de l'Asie, par analogie aux péridotites de la marge Galice [10,13], soit au niveau de la dorsale océanique à vitesse lente de l'océan Paléo-Téthys, par analogie aux péridotites de diverses rides actuelles (ride équatoriale médio-atlantique, ride indienne sud-ouest, ride atlantique-antarctique) [7,15,16,28]. Des recherches supplémentaires sont nécessaires pour préciser la nature des lherzolites résiduelles de la suture Anyemaqen. Mais la découverte de ce type de roche révèle néanmoins l'existence incontestable d'une croûte océanique paléozoïque sur cette transversale du Kunlun, qui pourrait bien constituer les restes de l'océan majeur entre Gondwana et Angara.

1. Introduction

Ophiolites in the Northeast Tibet are found in association with the Triassic Yushu–Jinshajiang River suture between the Qiangtang and the Songpan–Garze terranes, and with the Early Palaeozoic and Permo-Triassic Eastern Kunlun sutures, which separate the Songpan–Garze and the Kunlun (Qaidam) terranes (Fig. 1a). A crucial question for the geology of this region is: do sutures represent the remnants of the Palaeo-Tethyan Ocean?

Early studies in southern Tibet demonstrated that the Yarlung Tsangbo ophiolite belt could represent the suture zone between Eurasia and Gondwana [12]. However, palaeontological and stratigraphical evidence strongly suggest now that this boundary lies much further north. According to more recent studies, Gondwana-type sedimentary rocks with cold-water fossils such as Eurydesma and Lytrolasma occur much farther north of Tibet [31,32], even north of the Yushu–Jinshajiang River Suture, close to the south margin of Kunlun [30]. The same type of rocks also occurs in the easternmost part of the Tibetan Plateau [11,22]. The distribution of these sedimentary rocks suggests that most of the Tibetan Plateau was part of Gondwanaland and that the northern boundary between the Eurasian and Gondwana plates lies near the Kunlun Mountains.

Two sutures – the Early Palaeozoic Middle Kunlun suture and the Permo-Triassic South Kunlun (Anyemaqen) suture – are distinguished at the northern margin of the Tibetan Plateau in the eastern Kunlun area (Fig. 1a). The Middle Kunlun suture represents the oldest belt, and contains ophiolites of Cambrian age. These rocks crop out in the central part of eastern Kunlun, extend for at least a few hundred kilometres and are believed to reflect a small ocean basin [33]. South of it, the Anyemaqen suture extends nearly 1200 km and contains numerous ophiolitic blocks of Early Permian to Middle Triassic age and exotic Early Permian bioclastic limestone blocks in a matrix of the Triassic flysch [33].

The origin of the Anyemaqen ophiolites is debatable. Previously, the lavas from this suture were determined to be similar to within-plate tholeiites or plume-related mid-oceanic ridge basalts originated at a passive margin during Permian rifting [27]. The origin during a rifting event for Anyemaqen ophiolites has also been proposed by [24]. However, the later

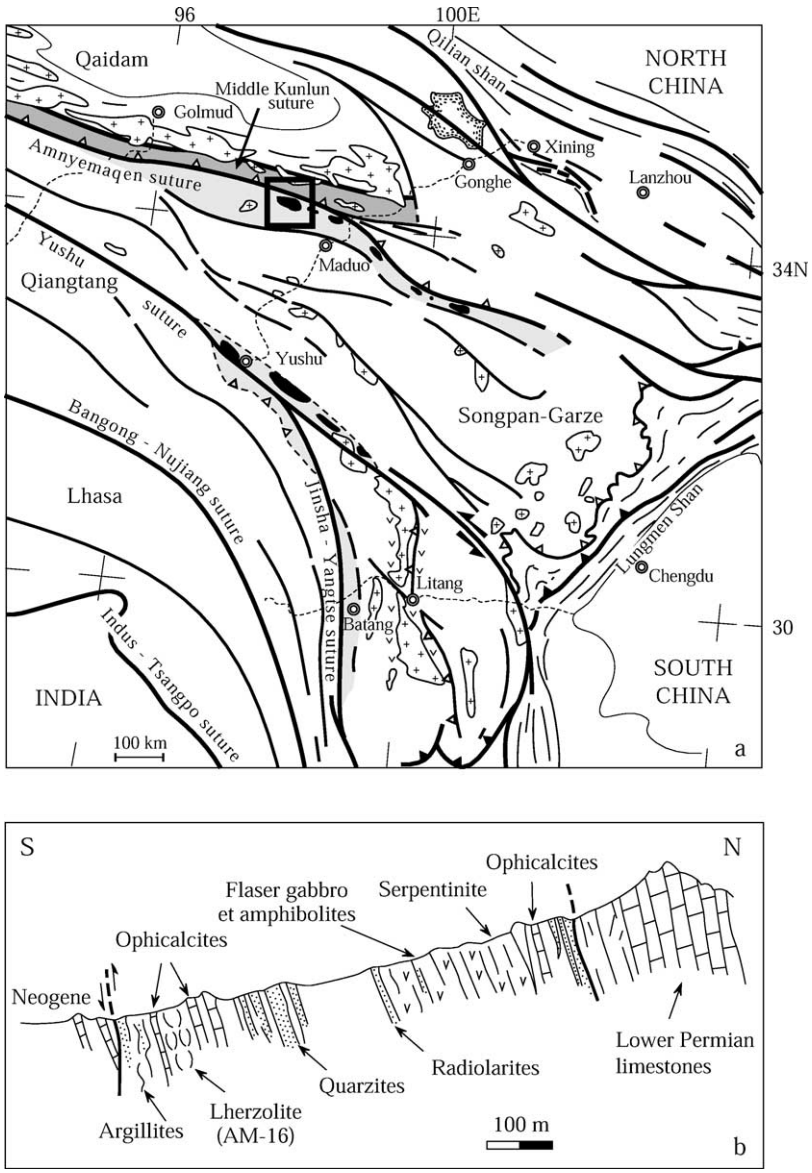

Fig. 1. (**a**) Tectonic sketch map of the Eastern Tibet area. Square indicates location of the examined ophiolite domain in the Anyemaqen suture. (**b**) Geological section of the ophiolites from the West Huashexia–South Tong Xi Tso Lake area.

Fig. 1. (**a**) Carte tectonique schématique du Tibet oriental. Le carré marque les affleurements d'ophiolites étudiées dans la suture Anyemaqen. (**b**) Coupe géologique de la série ophiolitique à l'ouest de Huashexia et au sud du lac Tong Xi Tso.

study has shown [33] that ophiolites from the Anyemaqen suture consist of volcanic rocks with geochemical affinities typical for the rocks originated at mid-oceanic ridge, oceanic islands and volcanic arcs. The belt was interpreted as the suture zone between Gondwana and Eurasia [33]. Obviously, the data concerning only volcanic rocks do not allow us to determine the nature of the ophiolites from the Anyemaqen suture and new data on the deeper parts of the ophiolitic section are needed.

We describe for the first time the chemical composition of the primary phases of peridotites sampled in the Anyemaqen suture.

2. Geological setting

The Anyemaqen suture trends to the east-southeast at 35°N latitude west of Xining, North Tibet (Fig. 1a). It is reactivated by the active Kunlun Fault, which separates the Kunlun Range from the Tibetan Plateau. The suture is characterized by the occurrence of radiolarites, pillow lava basalts, granodiorites, flaser gabbros, amphibolites and peridotites, which form individual bodies from less than 1 km^2 to 10 km^2. This association is typical of ophiolitic series found in the Alps or along the Iberia margin [1–3,19–21,23]. All these rocks, components of a dismembered ophiolitic sequence, crop out as imbricated tectonic lenses within the Kunlun fault zone. Blocks of neritic bioclastic Permian limestones, which represent marginal basin deposits, are also reported [6].

The studied geological section is located near the West Huashexia–South Tong Xi Tso Lake area (Fig. 1b). The series fall steeply to the north. The ophiolites are separated from Neogene sedimentary rocks to the south and from massive limestones to the north by two segments of the recent brittle Kunlun fault. The limestones contain benthic Foraminifera fossil remnants indicating internal platform environment, from which D. Vachard determined a Lower Permian age (Middle Asselian) *Sphaeroshwagerina shamovi* (1949) and *Rugosofusulina pandae* (1962), which have Angara affinity. The ophiolite sequence is composed mostly of peridotites and flaser gabbro-amphibolites. Lenses of ophicalcites, reddish argillites and radiolarites, locally recrystallized in quartzites, also occurred (Fig. 1b). Peridotites and gabbro-amphibolites are deformed into mylonites along narrow zones, which bound more preserved domains. The ophicalcites found among peridotites and gabbro-amphibolites are composed of magnesite tectonic breccias or magnesite-magnetite layered aggregates, which contain isolated crushed and euhedral Cr-spinel crystal relics and zones of Fe–Ni mineralisation.

3. The Anyemaqen peridotite

A well-preserved sample (AM-16) of peridotite from the ophiolitic section was discovered and selected for a detailed study (Fig. 1b). The peridotite is exceptionally weakly altered and contains about 5% serpentine, as determined from the optical microscope. It is consistent with loss on ignition (LOI) value in the whole-rock analysis (Table 1). The modal composition of the peridotite is $\leqslant$68% olivine (Ol), 25% orthopyroxene (Opx), $\geqslant$5% residual clinopyroxene (Cpx) and 2% Cr–Al spinel (Sp), corresponding to transition between a clinopyroxene-rich harzburgite and a clinopyroxene-poor spinel lherzolite.

The texture of the peridotite AM-16 is mylonitic. The large elongated Opx porphyroclasts have a preferred alignment, which defines the foliation of the rock. The matrix of the peridotite is composed of fine-grained, dynamically recrystallized Ol with rare grains of Cpx and amoeboid interstitial grains of Cr–Al Sp, elongated parallel to the rock foliation.

Orthopyroxene porphyroclasts (up to 1 cm long) are characterized by a maximum elongation ratio about 1:3–1:5. They are abraded by deformation and are plastically deformed by (100) glide, displaying undulose extinction, kink structures and exsolution lamellae of Cpx (Fig. 2A). The shear planes in porphyroclasts are usually oblique to the foliation in the rock that indicates non-coaxial deformation (Fig. 2B). The Opx porphyroclasts are often flanked by a mantle of tapering, recrystallized grain aggregates, of both Opx and Ol, developed by high stress recrystallization (Fig. 2B). In other cases, the Opx porphyroclasts display traces of resorption as a result of interaction with a low-silica content melt or fluid: most of the porphyroclasts are irregularly shaped and clearly replaced by neoblasts of Ol (up to 80–130 μm) and black interstitial Sp, occurring at the edges of deformed porphyroclasts (Fig. 2C). The composition of Opx slightly differs in porphyroclasts from $Wo_{2.01}En_{88.29}Fs_{9.7}$ to $Wo_{1.31}En_{88.36}Fs_{10.3}$ (Table 1).

Clinopyroxene occurs as sub-euhedral or irregular residual porphyroclasts (190–380 μm and very rarely up to 600 μm). Most of them are internally deformed, displaying undulose extinction and exsolution lamellae. Like the Opx porphyroclasts, the Cpx grains are transformed at their periphery in neoblasts

Table 1
Microprobe analyses of Ol, Cpx, Opx and Sp from the Anyemaqen peridotite (AM-16) (Cameca microprobe, 'Université Montpellier-2', Montpellier, France), and a whole rock analysis (wet chemistry, VIMS, Moscow)

Tableau 1
Analyses microsonde de Ol, Cpx, Opx et Sp de la péridotite d'Anyemaqen (AM 16) (microsonde Cameca, université Montpellier-2), et l'analyse de roche totale (VIMS, Moscou)

Sample mineral	AM-16 Ol-1 relic	AM-16 Ol-2 neoblast	AM-16 Cpx-1 core	AM-16 Cpx-1 rim	AM-16 Opx-1 with exsolution	AM-16 Opx-2 free of exsolution	Sample mineral	AM-16 Sp core	Sample rock	AM-16 peridotite
SiO_2	41.28	41.27	53.41	54.27	54.86	55.78	SiO_2	0.146	SiO_2	42.60
TiO_2	n.d.	n.d.	0.22	0.24	0.03	0.06	TiO_2	0.100	TiO_2	0.05
Al_2O_3	0.03	n.d.	3.86	1.96	5.50	4.41	Al_2O_3	50.032	Al_2O_3	1.79
Cr_2O_3	n.d.	n.d.	0.94	0.29	0.51	0.59	Cr_2O_3	17.614	FeO	5.46
Fe_2O_3	–	–	–	–	–	–	Fe_2O_3	1.787	Fe_2O_3	3.03
FeO*	9.71	9.93	2.15	2.28	6.71	6.36	FeO	13.166	MnO	0.16
MnO	0.23	0.30	0.10	0.13	0.00	0.17	MnO	0.237	MgO	40.16
MgO	50.01	49.37	16.34	17.53	32.22	32.50	MgO	17.538	CaO	2.25
CaO	0.04	0.01	24.32	23.98	0.66	1.03	NiO	–	Na_2O	0.06
Na_2O	–	–	–	–	0.26	0.06			K_2O	0.07
Total	101.28	100.87	101.34	100.67	100.75	100.96	Total	100.441	P_2O_5	0.01
							FeO*	14.774	H_2O	0.04
									LOI	4.68
	O = 4		O = 6		O = 6			O = 32		
Si	1.032	1.038	1.929	1.971	1.926	1.950	Si	0.031	Total	100.36
Ti	–	–	0.006	0.007	0.001	0.002	Ti	0.016	CO_2	0.15
Al	0.001	–	0.164	0.084	0.227	0.182	Al	12.653		
Cr	–	–	0.027	0.008	0.014	0.016	Cr	2.988	Rb	5.000
Fe^{3+}	–	–	–	–	–	–	Fe^{3+}	0.288	Ba	46.000
$Fe^{2+}*$	0.203	0.209	0.065	0.069	0.197	0.186	Fe^{2+}	2.362	Sr	360.000
Mn	0.005	0.006	0.003	0.004	0.000	0.005	Mn	0.043	Cr	2216.200
Mg	1.862	1.849	0.879	0.948	1.685	1.692	Mg	5.607	Ni	175.000
Ca	0.001	0.000	0.940	0.933	0.025	0.039	Ni	–	Zn	8.000
Na	0.000	0.000	0.000	0.000	0.018	0.004				
Z	1.032	1.038	2.099	2.061	2.154	2.133	A	8.012		
XY	2.071	2.064	1.914	1.962	1.939	1.942	B	15.976		
Wo			0.499	0.478	0.013	0.020	Cr	0.188		
En			0.466	0.486	0.884	0.883	Al	0.794		
Fs			0.034	0.036	0.103	0.097	Fe^{3+}	0.018		
Mg#	0.902	0.899	0.931	0.932	0.895	0.901	Mg#	0.704		
							Cr#	0.191		
							Fe#	0.018		

Note : FeO* total iron as FeO ; $Fe^{2+}*$ total iron as Fe^{2+} ; Fe^{2+} and Fe^{3+} for spinel are calculated from total iron on the basis of AB_2O_4 stoichiometry ; Mg # $Mg/(Mg + Fe^{2+})$; Cr # $Cr/(Cr + Al)$; Fe# $Fe^{3+}/(Cr + Al + Fe^{3+})$.

FeO* fer total pour FeO ; $Fe^{2+}*$ fer total pour Fe^{2+} ; Fe^{2+} and Fe^{3+} de Sp sont calculés à partir du fer total sur la base stœchiométrique AB_2O_4 ; Mg# $Mg/(Mg + Fe^{2+})$; Cr# $Cr/(Cr + Al)$; Fe# $Fe^{3+}/(Cr + Al + Fe^{3+})$.

of Ol and Sp (Fig. 2D and E). The composition of Cpx in cores of the residual host grains differs slightly from that in its rims (Fig. 3d). Cpx has a composition $Wo_{49.92}En_{46.64}Fs_{3.4}$ in the cores and is characterized by higher contents of Al_2O_3, Cr_2O_3, CaO and slightly lower TiO_2 compared to Cpx in the rims ($Wo_{47.83}En_{48.62}Fs_{3.6}$) (Table 1). The decrease of Cr and Al contents in the rim compared to the core suggests *subsolidus* re-equilibration at lower temperature with formation of additional Sp in a closed system.

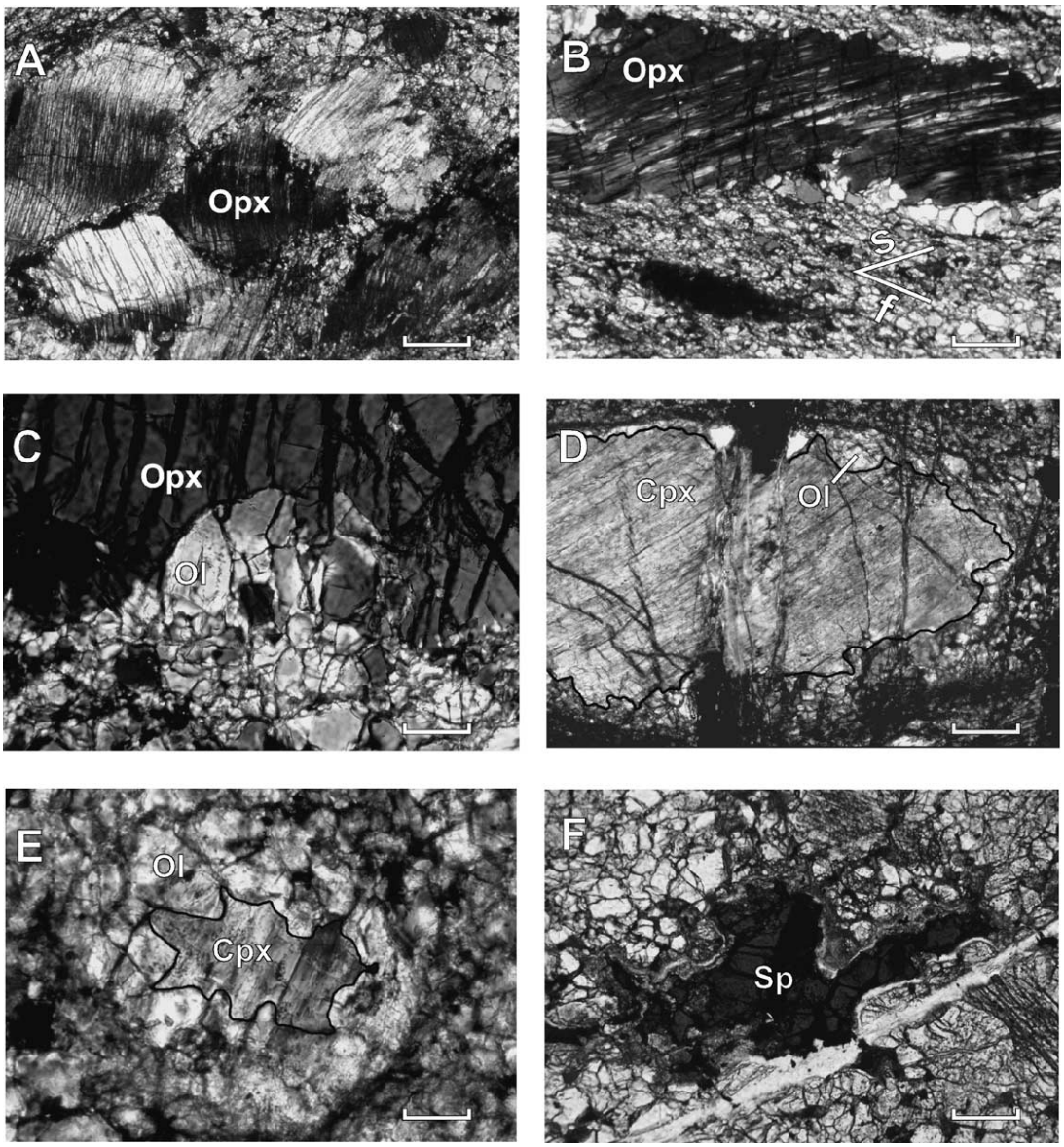

Fig. 2. Photomicrographs of main mineral phases in the Anyemaqen peridotite sample (AM-16). **A.** Opx porphyroclast displaying kink structure, undulose extinction and lamellae exsolution of Cpx. Scale bar is 350 μm. **B.** Mantled elongated Opx porphyroclast sheared obliquely at 39° (s) relative to mylonitic foliation (f) in the matrix and flanked by tapering grain aggregates both of Opx and Ol. Scale bar is 161 μm. **C.** Resorption of Opx porphyroclast by Ol and Sp neoblasts. Scale bar is 81 μm. **D–E.** Relic Cpx grains resorbed by Ol and Sp neoblasts at the edges (**D**) and nearly completely (**E**). The scale bars are 161 μm (**D**) and 42 μm (**E**). **F.** The amoeboid irregular grain of Cr–Al Sp surrounded by late rims of magnetite and serpentine. Scale bar is 139 μm. Fig. 2C is taken under plane-polars, all others under crossed-polars.

Fig. 2. Microphotographies des phases minérales de la péridotite d'Anyemaqen (AM16). **A.** Porphyroclaste d'Opx avec bande de pliage, extinction ondulante, et lamelle d'exsolution de Cpx. Échelle 350 μm. **B.** Structure cœur–bordure dans un porphyroclaste étiré d'Opx, cisaillé à 39° (s) par rapport au plan de foliation mylonitique (f). Échelle : 161 μm. **C.** Résorption de porphyroclaste d'Opx par les néoblastes d'Ol et Sp. Échelle : 81 μm. **D**–**E**. Les grains de Cpx résiduel sont substitués par les néoblastes d'Ol et Sp en bordure (**D**) ou presque totalement (**E**). Échelle : 161 μm (**D**) et 42 μm (**E**). **F.** Grain amiboïde de Cr–Al Sp entouré de bordures secondaires de magnétite et serpentine. Échelle : 139 μm. Photographies en polariseurs croisés, excepté photo **C** en polariseurs plans.

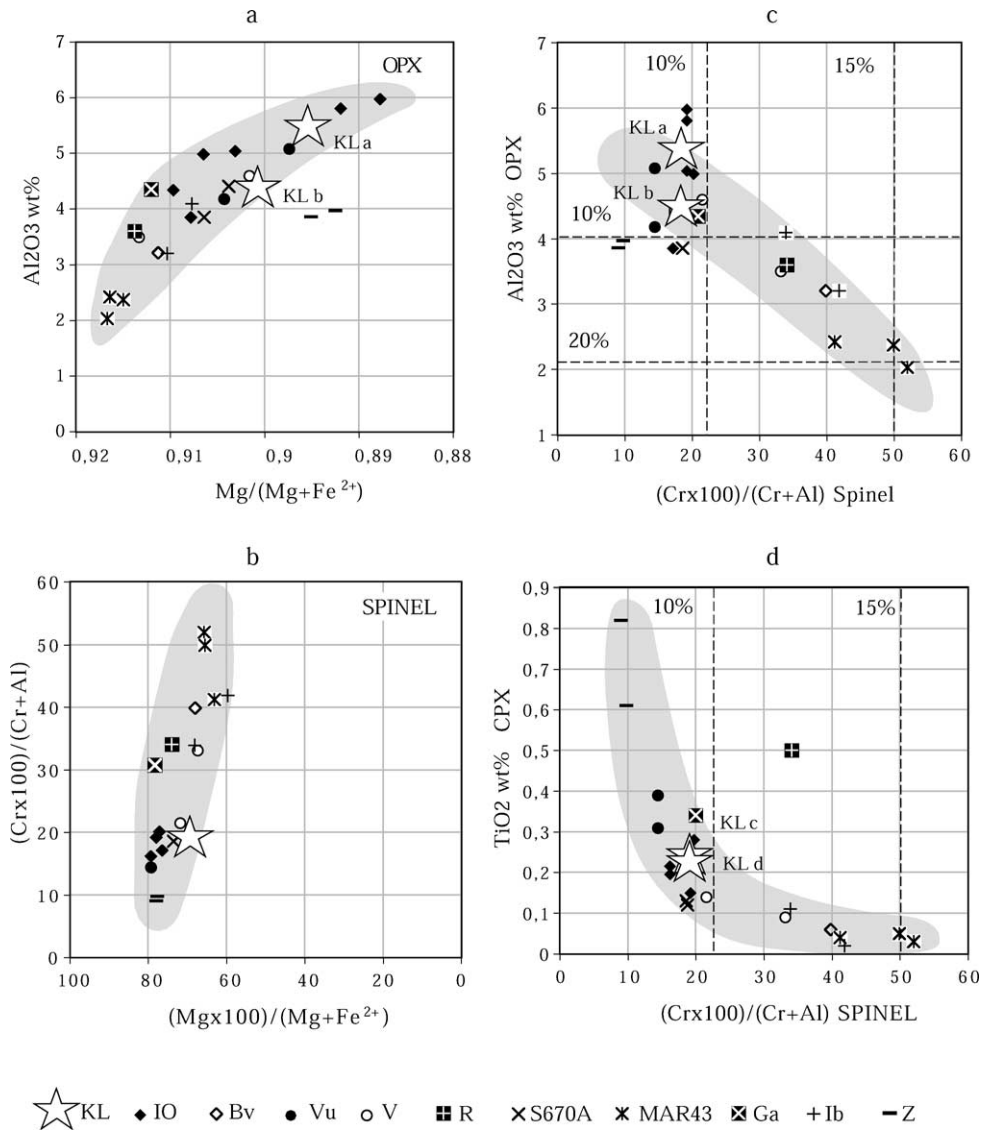

Fig. 3. Diagrams showing chemical composition of Opx, Cpx and Sp from the Anyemaqen peridotite AM-16 (**KL**). Shadow area indicates average trend of the ocean-floor residual peridotites. **IO**, Islas Orcadas and Shaka F.Z.; **Bv**, Bouvet F.Z.; **Vu**, Vulcan F.Z.; **V**, Vema F.Z.; **R**, Romanche F.Z.; **S670A**, Site 670A; **MAR43**, 43°N Mid-Atlantic Ridge; **Ga**, Galicia margin, Site 637A; **Ib**, Iberia margin, Site 899B; **Z**, Zabargad Island of Red Sea. The data are taken from [4,5,8–10,13,15,16,28,29]. **KLa** and **KLb** indicate the Opx composition from the AM-16 peridotite with and free of Cpx exsolution, respectively; **KLc** and **KLd** indicate the Cpx composition in rim and in core, respectively. Degree of melting at Fig. 3c and d is shown after [14].

Fig. 3. Diagramme des compositions chimiques des Opx, Cpx et Sp de la péridotite d'Anyemaqen (AM-16) (**KL**). Les domaines ombrés correspondent à la moyenne des péridotites océaniques résiduelles. **IO**, Islas Orcadas et Shaka F.Z. ; **Bv**, Bouvet F.Z. ; **Vu**, Vulcan F.Z. ; **V**, Vema F.Z. ; **R**, Romanche F.Z. ; **S670A**, site 670A ; **MAR43**, 43°N ride médio-atlantique ; **Ga**, marge Galice, Site 637A ; **Ib**, marge Ibérie, Site 899B ; **Z**, île de Zabargad, mer Rouge. Les données sont issues des références [4,5,8–10,13,15,16,28,29]. **KLa** et **KLb** indiquent la composition Opx avec ou sans exsolution de Cpx respectivement. **KLc** et **KLd** indiquent respectivement la composition des Cpx en bordure ou au cœur. Le degré de fusion sur la Fig. 3c et d est donné d'après [14].

Olivine forms fine-grained groundmass of the peridotite and occurs as elongated grains (about 80 μm) or polycrystalline ribbons (170 μm, up to 600 μm) and as small dynamically recrystallized olivine neoblasts (about 20–30 μm). The Ol ribbons are elongated with aspect ratio varying from 3:1 to 7:1 and aligned parallel to the foliation defined by Opx and Sp. The relic Ol grains display subgrain boundaries and undulose extinction and replaced at the edges by the Ol neoblasts. The Ol composition varies from Fo_{90} in relic grains to Fo_{89} in neoblasts (Table 1).

Spinel occurs in two morphologies. One phase is represented by green–brown irregular amoeboid grains (up to 1 mm long) elongated parallel to the Opx and Ol ribbon foliations (Fig. 2F). The other phase of Sp is observed as smaller black interstitial grains (about 10 μm) dispersed in the olivine matrix (Fig. 2C, E and F). The composition of spinel elongated amoeboid grains in lherzolite is characterized by high Al_2O_3 contents (Table 1) and plots on a Cr# vs. Mg# diagram close to those from oceanic residual peridotites, determined by [9] as being of a 'high-alumina type' (Fig. 3b).

Secondary phases: two late systems of serpentine veins occur in the peridotites, parallel to or crosscutting the mylonitic foliation at 35–40° or 90°. Serpentine minerals are optically determined as chrysotile and lizardite, which are laced and streaked with dusty magnetite. The Opx and Cpx porphyroclasts crossed by serpentine veins are partially replaced by bastite lizardite (Fig. 2D). Sp grains are surrounded by inner rim of magnetite and outer rim of lizardite, which is usually spatially connected to the main phase of serpentine veins (Fig. 3F).

4. Discussion and conclusions

The textural, mineralogical and modal characteristics of studied peridotites from the Anyemaqen suture indicate their affinity with ultramafic tectonites, as defined by [26], whereas the typical features of magmatic cumulates in the peridotites are lacking. The peridotite belongs most likely to the upper mantle.

Observed mineral chemistry of the Anyemaqen spinel lherzolite shows relatively high abundances of the magmaphile elements Fe, Al, Ti in the main primary mineral phases. The exhumed mantle rock displays a moderate percentage of melting, which corresponds to less than 10% by comparison with the experimental studies on the Tinaquillo peridotite (Fig. 3c and d) [14]. Its composition mostly resembles that of the less depleted oceanic residual peridotites, collected in fracture zones or rift valley of slow spreading ridge segments (South-West Indian Ridge, Atlantic-Antarctic Ridge, Equatorial Mid-Atlantic Ridge) [7, 15,16,28] and in the Galicia passive continental margin [10,13] (Fig. 3).

Mylonite texture, marked by plastically deformed Opx porphyroclasts, elongated green-brown Cr–Al Sp grains and Ol ribbons, indicates that this rock underwent a plastic shear deformation event. The obliquity of the shear plane in Opx porhyroclasts with respect to the foliation suggests that the deformation was achieved by non-coaxial shear flow. The significant difference in size of large Opx porphyroclasts and small olivine neoblasts in the matrix suggests that the deformation developed by plastic flow at low temperatures 800–1000 °C [25].

The Anyemaqen peridotite underwent a subsolidus reequilibration, which probably occurred during the ductile shear deformation and appears to be active after it, because both kinked Opx and Cpx porphyroclasts are resorbed at their edges by secondary Ol and small black Sp neoblasts. The mineral assemblage in the rock suggests that the reequilibration occurred under conditions of temperature and pressure appropriate to spinel peridotite facies. We therefore propose that a mineralogical reaction took place, consuming orthopyroxene and clinopyroxene, and formation of olivine + spinel ± melt [17,18].

Textural and chemical characteristics of residual peridotites from the Anyemaqen suture are consistent with two possible hypotheses for their origin. The mantle material could have been emplaced at a shallow depth during incipient rifting on the passive Asian margin, similar to peridotites reported from the Galicia passive margin [10,13] Alternatively, we suggest that the residual lherzolites represent the mantle material uplifted at slow spreading ridge setting in Palaeo-Tethyan Ocean, similar to peridotites occurring presently in the mid axial rift valley of the Equatorial Mid-Atlantic Ridge, South-West Indian Ridge, Atlantic-Antarctic Ridge [7,15,16,28]. Further researches are needed to make a definite choice between these two alternatives.

Acknowledgements

We are grateful to J. Girardeau and an anonymous reviewer for their valuable suggestions, resulting in substantial improvements to the manuscript, and to J. Dercourt for able editorial support. We would like to thank F. Boudier for fruitful discussions, C. Merlet for help in carrying out the electron microprobe analyses in Montpellier, G.N. Avdeeva, G.M. Kolesov, D.Yu. Sapognikov for the bulk-rock analyses realized in Moscow, D. Vachard for age determination of Foraminifera fossil remnants. Special thanks to A. Delplanque and J. Montesinos for assistance in preparing the illustrations. Funding has been provided by INSU–CNRS programs and the grant 'Nadegda' of the Russian Foundation for Basic Research (1996).

References

[1] D. Bernoulli, Ancient continental margins of the Tethyan Ocean, in: Geology of Passive Continental Margins: History, Structure and Sedimentologic Record (with Special Emphasis on the Atlantic Margin), in: AAPG Continuing Education Course Note Series, Vol. 19, 1981, pp. 1–36.

[2] D. Bernoulli, M. Lemoine, Birth and early evolution of the Téthys; the overall situation, in: Géologie des chaînes alpines issues de la Tethys/Geology of the Alpine chains born of the Tethys, Mém. BRGM 115 (1980) 168–179.

[3] D. Bernoulli, H. Weissert, Sedimentary fabrics in Alpine ophicalcites, South Pennine Arosa Zone, Switzerland, Geology (Boulder) 13 (11) (1985) 755–758.

[4] M.-O. Beslier, G. Cornen, J. Girardeau, Tectono-metamorphic evolution of the peridotites from the ocean/continent transition of the Iberia abyssal plain margin, in: R.B. Whimarsh, D.S. Sawyer, A. Klaus, D.G. Masson (Eds.), Proc. ODP, Sci. Results, Vol. 149, College Station, TX (Ocean Drilling Program), 1996, pp. 397–412.

[5] E. Bonatti, G. Ottonello, P.R. Hamlyn, Peridotites from the Island of Zabargad (St. John), Red Sea: petrology and geochemistry, J. Geophys. Res. 91 (1986) 599–631.

[6] M. Brunel, F. Boudier, J. Malavieille, P. Tapponnier, Petrographic characters of peridotites from Anyemaqen and Yangtze sutures: geodynamic implication, in: Symposium on Uplift, Deformation and Deep Structure of Northern Tibet (Abstracts), La Grande Motte, France, 1995, pp. 21–22.

[7] M. Cannat, T. Juteau, E. Berger, Petrostructural analysis of the Leg 109 serpentinized peridotites, in: R. Detrick, J. Honnorez, W.B. Bryan, T. Juteau, et al. (Eds.), Proc. ODP, Init. Rep., Vol. 106–109, College Station, TX (Ocean Drilling Program), 1990, pp. 47–57.

[8] G. Cornen, M.-O. Beslier, J. Girardeau, Petrologic characteristics of the ultramafic rocks from the ocean/continent transition in the Iberia abyssal plain, in: R.B. Whimarsh, D.S. Sawyer, A. Klaus, D.G. Masson (Eds.), Proc ODP, Sci. Results, Vol. 149, College Station, TX (Ocean Drilling Program), 1996, pp. 377–395.

[9] H.J.B. Dick, T. Bullen, Chromian spinel as a petrogenetic indicator in abyssal and alpine-type peridotites and spatially associated lavas, Contrib. Mineral. Petrol. 86 (1984) 54–76.

[10] C.A. Evans, J. Girardeau, Galicia margin peridotites: undepleted abyssal peridotites from the North Atlantic, in: G. Boillot, E.L. Winterer, et al. (Eds.), Proc. ODP, Sci. Results, Vol. 103, College Station, TX (Ocean Drilling Program), 1988, pp. 195–207.

[11] Y.N. Fan, A division of biogeographical provinces by Permo-Carboniferous corals in Xizang, China, Contrib. Geol. Qinghai-Xizang (Tibet) Plateau 16 (1985) 87–106 (in Chinese with English abstract).

[12] A. Gansser, The significance of the Himalayan suture zone, Tectonophysics 62 (1980) 37–52.

[13] J. Girardeau, C.A. Evans, M.-O. Beslier, Structural analysis of plagioclase-bearing peridotites emplaced at the end of continental rifting: Hole 637A, ODP Leg 103 on the Galicia margin, in: G. Boillot, E.L. Winterer, et al. (Eds.), Proc. ODP, Sci. Results, Vol. 103, College Station, TX (Ocean Drilling Program), 1988, pp. 209–223.

[14] A.L. Jaques, D.H. Green, Anhydrous melting of peridotite at 0–15 kb pressure and the genesis of tholeitic basalts, Contrib. Mineral. Petrol. 73 (1980) 287–310.

[15] K.T. Johnson, H.J.B. Dick, N. Shimizu, Melting in the oceanic upper mantle: an ion microprobe study of diopsides in abyssal peridotites, J. Geophys. Res. 95 (1990) 2661–2678.

[16] T. Juteau, E. Berger, M. Cannat, Serpentinized, residual mantle peridotites from the M.A.R. Median Valley, ODP Hole 670A (21°10′N, 45°02′W, LEG 109): primary mineralogy and geothermometry, in: R. Detrick, J. Honnorez, W.B. Bryan, T. Juteau, et al. (Eds.), Proc ODP, Init. Rep., Vol. 106–109, College Station, TX (Ocean Drilling Program), 1990, pp. 27–45.

[17] P.B. Kelemen, Reaction between ultramafic rock and fractionating basaltic magma. I. Phase relations, the origin of calc-alkaline magma series, and the formation of discordant dunite, J. Petrol. 31 (1990) 51–98.

[18] P.B. Kelemen, M.S. Ghiorso, Assimilation of peridotite in calc-alkaline plutonic complexes: evidence from the Big Jim complex, Washington Cascades, Contrib. Mineral. Petrol. 94 (1986) 12–28.

[19] Y. Lagabrielle, M. Lemoine, Alpine, Corsican and Apennine ophiolites: the slow-spreading ridge model, C. R. Acad. Sci. Paris, Ser. IIa 325 (1997) 909–920.

[20] Y. Lagabrielle, M. Cannat, Alpine Jurassic ophiolites resemble the modern central atlantic basement, Geology 18 (1990) 319–322.

[21] M. Lemoine, G. Boillot, P. Tricart, Ultramafic and gabbroic ocean floor of the Ligurian Tethys (Alps, Corsica, Apennines): in search of a genetic model, Geology 15 (1987) 622–625.

[22] Z.Q. Liu, X. Xu, G.T. Pan, T.Z. Li, G.M. Yu, X.G. Yu, X.Z. Jiang, G.Y. Wei, C.S. Wang, Tectonics and Evolution of the Qinghai and Tibet Plateau, Geological Publishing House, Beijing, 1990 (in Chinese with English abstract).

[23] G. Manatschal, D. Bernoulli, Rifting and early evolution of ancient ocean basins: the record of the Mesozoic Tethys and the Galicia-Newfoundland margins, in: J. Erzinger, J.-C. Sibuet, M. Talwani (Eds.), Volcanic Margins, Mar. Geophys. Res. 20 (4) (1998) 371–381.

[24] M. Mattauer, J. Malavieille, S. Calassou, J. Lancelot, F. Roger, Z. Hao, Z. Xu, L. Hou, The Songpan-Garse Triassic belt of West Sechuan and Eastern Tibet: a decollement fold belt on passive margin, C. R. Acad. Sci. Paris, Ser. II 314 (1992) 619–626.

[25] A. Nicolas, Structure and petrology of peridotites: clues to their geodynamic environment, Rev. Geophys. 24 (1986) 875–895.

[26] A. Nicolas, Structures of the Ophiolites and Dynamics of Oceanic Lithosphere, Kluwer Academic, London, 1989.

[27] J.A. Pearce, D. Wanming, The ophiolites of the Tibetian Geotraverses, Lhasa to Golmud (1985) and Lhasa to Kthmandu (1986), Phil. Trans. Roy. Soc. London A 327 (1988) 215–238.

[28] M. Prinz, K. Keil, J.A. Green, A.M. Reid, E. Bonatti, J. Honnorez, Ultramafic and mafic dredge samples from the equatorial Mid-Atlantic Ridge and fracture zones, J. Geophys. Res. 81 (1976) 4087–4103.

[29] T. Shibata, G. Thompson, Peridotites from the Mid-Atlantic Ridge at 43°N and their petrogenetic relation to abyssal tholeiites, Contrib. Mineral. Petrol. 93 (1986) 144–159.

[30] D.L. Sun, On the Permian biogeographic boundary between Gondwana and Eurasia in Tibet. China as the eastern section of the Tethys, Palaeogeogr. Palaeoclimatol. Palaeoecol. 100 (1993) 59–77.

[31] N.W. Wang, The rise of Gondwana research in China and some key problems on paleobiogeography related to plate tectonics, Bull. Chin. Acad. Geol. Sci. I (10) (1984) 103–115 (in Chinese with English abstract).

[32] X.C. Xiao, T.D. Li, G.Q. Li, C.F. Chang, X.C. Yuan, Tectonic Evolution of the Crust-upper Mantle of the Qinghai-Xizang (Tibet) Plateau: General Review, Geological Publishing House, Beijing, 1988 (in Chinese with English abstract).

[33] J.S. Yang, P.T. Robinson, C.F. Jiang, Z.Q. Xu, Ophiolites of the Kunlun Mountains, China and their tectonic implications, Tectonophysics 258 (1996) 215–231.